Original Article

Cite This: Colloid & Nanoscience Journal 2(3) (2024) 336-356.

CNJ.araku.ac.ir

Fabrication and characterization of PES based nanofiltration membrane using bio-inspired iron (III)-dopamine nanoparticles

Fahime Parvizian[1]*, Mojgan Ebrahimi[a], Samaneh Bandehali[2]*, Arash Alimadadi[a]

Received: 2024-11-17
Revised: 2025-01-12
Accepted: 2025-01-17
DOI: 10.61186/CNJ.2.3.336

[1]Department of Chemical Engineering, Faculty of Engineering, Arak University, Arak 38156-8-8349, Iran
[2]Department of Mechanical Engineering, Ayatollah Boroujerdi University, Boroujerd 69199-69737, Iran

Abstract

This paper presents a study on the modification of nanofiltration membranes with bio-inspired iron (III)-dopamine nanoparticles in a polymer solution. The membranes were produced using the immersion precipitation technique with the incorporation of dopamine, polyvinyl pyrrolidone, and dimethylacetamide. The study evaluated the properties of the nanocomposite membranes, including water content, surface morphology, and their performance was characterized through SEM, contact angle goniometry, pure water flux, and rejection of NaCl and humic acid. The findings revealed that membranes containing 0.1 wt.% bio-inspired iron (III)-dopamine nanoparticles exhibited the best overall performance, with enhanced hydrophilicity, anti-fouling properties, and salt rejection efficiency. This optimal concentration also minimized fouling and improved the flux recovery ratio compared to other concentrations, highlighting its potential for water treatment applications.

Keywords: Nanofiltration membrane, Water treatment, Bio-inspired iron (III)-dopamine nanoparticles, Anti-fouling properties

1. Introduction

In modern technologies, industries are increasingly focused on practical and efficient separation processes for different substances. Separation and purification are often necessary for lengthy production processes. Industries frequently need to separate the components of raw materials to produce products that do not create pollutants that can enter water and air. Thus, the importance of separation processes for healthy water shortage is more evident than ever before, considering the significance of industries and the environment. For instance, pollution poses a threat to the planet, causing major crises and creating a need for methods to provide clean and healthy water. Separation methods can be categorized into three groups: separation by mass transfer, separation within one phase, and separation by chemical reaction. In the separation by mass transfer, an agent can form a second phase made of energy or mass, or both. Due to the issue of increasing energy prices and the development of the energy crisis, researchers are paying significant attention to this matter [1]. Separating and purifying materials is an energy-intensive process that requires identifying the active groups in a mixture. To reduce energy consumption, researchers are developing alternative methods. One such method is the use of nanofiltration membranes or composite membranes with nanoparticles, which provide higher selectivity in separation. These membrane processes are relatively new and are evolving rapidly. They offer high controllability and flexibility during operations, and their inherent properties, such as yield and process simplicity, make them highly suitable for separating constituent parts. They also have high environmental compatibility, low energy consumption requirements, and higher stability of separation conditions. As a result, membrane processes are increasingly used in various industrial processes, such as wastewater treatment and water desalination [1,2]. In modern technologies, industries are increasingly focused on practical and efficient separation processes for different substances. Separation and purification are often necessary for lengthy production processes. One of the crucial processes is the separation and purification of materials, particularly in industries aiming to mitigate environmental pollution and ensure cleaner water and air. Recent advances in membrane technology have led to the

Corresponding author: Fahime Parvizian, Samaneh Bandehali
Email: f-parvizian@araku.ac.ir, s.bandehali@abru.ac.ir

development of nanofiltration membranes, which offer unique advantages such as high selectivity, energy efficiency, and environmental compatibility. These membranes have been extensively studied for water and wastewater treatment, with particular attention to improving their antifouling properties and separation efficiency. Nanotechnology has significantly contributed to this progress by enabling the design of functionalized nanoparticles that enhance membrane performance.

Bio-inspired nanoparticles, such as iron(III)-dopamine nanoparticles, have garnered considerable interest due to their exceptional properties, including high adhesion, biocompatibility, and resistance to fouling. For example, Li et al. (2012) [3] utilized iron(III)-dopamine nanoparticles in polymer-inorganic hybrid membranes for gas separation, demonstrating their potential to enhance membrane hydrophilicity and selectivity. Similarly, other studies have explored the incorporation of bio-inspired nanoparticles into membranes to improve water affinity, flux, and anti-fouling characteristics. Despite these advancements, the application of bio-inspired iron(III)-dopamine nanoparticles in nanofiltration membranes for water treatment remains relatively unexplored. Previous research has primarily focused on using these nanoparticles in gas separation or other hybrid systems. This study seeks to fill this gap by investigating the impact of bio-inspired iron(III)-dopamine nanoparticles on the performance of polyethersulfone (PES) membranes. The aim is to evaluate their influence on hydrophilicity, antifouling properties, and separation efficiency, thereby contributing to the development of advanced nanofiltration membranes for water treatment applications.

Nanotechnology involves making changes to materials at the nanoscale, which has led to the development of new materials, structures, and devices. Advances in science and engineering have allowed for the creation of nanosorbents, nanocatalysts, biologically active nanoparticles, catalytic membranes with nanostructures, magnetic nanoparticles, and other nanomaterials that can address issues such as poor water quality. The concept of nanotechnology was first introduced by Richard Feynman in 1959, and since then, many research studies on nanotechnology have been conducted. Implementing nanotechnology in industries is becoming increasingly important, as it can lead to water treatment technologies that are both cost-effective and durable. Moreover, nanotechnology is a green technology that can help control and prevent environmental pollution [4]. Nanotechnology can be used in two areas for water purification. Firstly, it can produce electrodes with a large surface area by placing carbon nanotubes together and using 10 times less energy than reverse osmosis and 100 times less energy than distillation to desalinate seawater. Secondly, nano composites can be produced and their structure can be improved to achieve better performance in removing water pollutants. One important application of nano technology is nano filtration, which is a relatively new process that has been developed since the mid-80s. The first application of it dates back to the second half of the 1980s. The first nano filtration membrane was cellulose acetate membranes that were very effective in removing salt. However, they needed improvement in terms of water flow rate, chemical and temperature stability. It has applications in various sectors including dams, protection of water pipelines, water and wastewater treatment, water softening and more. It is predicted that by 2050, nano technology, along with biotechnology and information technology, will create a revolution in human life [5,6].

Nanofiltration membranes are made up of two layers: a protective layer and an active layer. The protective layer acts as a support to protect against system pressure and has pore diameters larger than 50 nanometers, while the active layer is responsible for separation and has pore diameters in the nanometer scale. These membranes selectively separate homogeneous phases and prevent impurities from passing through. There are two removal mechanisms at work in nano filtration membranes: physical removal and electrostatic repulsion. The latter mechanism is due to the negative charge on the surface of the membranes, which repels salts through the electrostatic force of anions. Nanofiltration membranes can be produced through polymerization in a common phase or phase change [7]. Many factors, such as environmental conditions, can affect the performance of nanofiltration membranes. Some important changes in this area include: For example, in a system with a decrease in feed pH, amino groups on the membrane surface are converted to R3HN, which leads to an increase in water affinity and flux [8]. Sometimes, fluctuations in pH in a fluid can have different effects on the removal of contaminants, or no effect at all. Also, as the cross-flow velocity increases, the flux rate increases because the layers that cause fouling on the membrane are removed at higher speeds. It should be noted that the maximum cross-flow velocity for each membrane is different and depends on the mechanical resistance of the desired membrane, element concentration, and system hardware. Working at high speeds causes early membrane failure in the modulus of elasticity [9]. In 2012, Yi Fan Li and his colleagues used iron-

dopamine nanoparticles to make hybrid polymer and inorganic membranes that consist of a continuous polymer phase and a dispersed filler phase. Among the various chemical branches derived from bio-hybrids, the chemistry of iron-rich adhesive shellfish has sparked considerable research interest. Due to oxidation and cross-linking of iron to dopant units, protein chains can act as exceptional underwater adhesives. In fact, in the presence of oxidants, small molecules with both a catechol group and an amino group, such as dopamine, can accumulate in nanoparticles and almost adhere to different surfaces due to multiple reactions [3]. In 2012, Daryaei and his colleagues conducted a study on the preparation of a nanocomposite membrane based on polyether sulfone. In this study, the effect of adding different concentrations of poly aniline/iron oxide nanoparticles to remove copper ions from water and the performance of polyether sulfone membranes were investigated. Finally, the optimal amount of these nanoparticles, which had the greatest effect on membrane performance, was obtained. Evaluations showed that the least amount of fouling occurred at a weight concentration of 1.0% of nanoparticles. Therefore, a weight concentration of 1.0% of poly aniline/iron oxide nanoparticles was selected as the optimal concentration. A membrane containing 1.0% weight of poly aniline/iron oxide nanoparticles showed the highest copper ion separation rate of about 65%, and the lowest water flux rate was also related to this membrane. The reason for this is the placement of nanoparticles in the surface cavities of the membrane during the phase inversion process in membrane production [11]. In 2014, Zeynini and his colleagues conducted a study to produce a high-flux nano filtration membrane using iron oxide nanoparticles coated with methyl carboxyl chitosan to remove color from water, and then evaluated the performance of this membrane at different concentrations of nanoparticles. Compared to membranes made from pure polyether sulfone, these membranes showed better water affinity and had a higher flux rate than membranes made from pure polyether sulfone. Finally, as the results of this study, adding nanoparticles at lower concentrations can increase water flux, separation percentage, and membrane resistance to fouling compared to samples without nanoparticles [12]. In 2016, a study by Jingguk Kim and his colleagues used iron-dopamine nanoparticles in a polyethylene glycol matrix with nanometer thickness to create a continuous and continuous set of polymer hybrid membranes for gas separation improvement [13]. In a study conducted by Bagheripour and his colleagues in 2016, a mixed matrix membrane of polyethersulfone with iron oxide and nickel nanoparticles was prepared. The effect of the concentration of iron oxide and nickel nanoparticles in the casting solution on the structure and performance of the membrane was investigated. Scanning electron microscopy images showed that the size of the empty spaces in the membrane layer increased with the increase of additive concentrations. The results showed that increasing the concentration of iron oxide and nickel nanoparticles from 0 to 0.1% weight in the membrane matrix reduced the contact angle from 63 to 43 degrees, and with an increase in particle concentration to 1% weight, it increased again to 56 degrees. Generally, salt permeability improved with increasing nanoparticle concentration. Nanocomposite membranes have better anti-fouling capacity compared to virgin polyethersulfone membranes [14]. In 2019, Kolyon and his colleagues successfully synthesized magnetic iron oxide nanoparticles using 3-aminopropyl triethoxy silane and dendrimer and then added a malamine-based amine to the polyethersulfone membrane. The membranes were made by the phase inversion method. The pure water flux of the mixed polyethersulfone membranes increased significantly due to their higher water affinity compared to their pure state. Results of resistance factors against fouling, including reversible fouling, irreversible fouling, and total fouling, showed that the membrane with 0.5% weight of nanoparticles was the best anti-fouling membrane. Additionally, compared to all other membranes produced, it showed the highest water affinity, anti-fouling, and permeability properties [15]. In 2019, Bagheripour and his colleagues modified the surface of a polyethersulfone nanofiltration membrane with polyvinyl alcohol and iron oxide nanoparticles through a crosslinking reaction with glutaraldehyde. The results showed that the pure water flux, porosity, and average pore size were reduced. The contact angle of the water was slightly lower due to the hydrophilic nature of the nanoparticles. Filtration of milk solution showed the best anti-fouling performance for the modified membrane with 2% weight of nanoparticles [16]. In 2020, Moradi and his colleagues prepared polyethersulfone-based nanofiltration membranes using the phase inversion method and iron oxide nanoparticles. The results showed that the porosity and average pore size of the modified membrane increased compared to the pure membrane. The pure water flux was significantly improved at 0.5% weight of iron oxide and 0.3% weight of sodium citrate. The highest salt rejection was 68%, while for the dense membrane, it was 61% [17]. In 2020, Ansari and his colleagues used 8-hydroxyquinoline to modify iron oxide nanoparticles and prepare a mixed matrix membrane based on polyethersulfone using the phase inversion method. After conducting the necessary tests, the results showed that the water contact angle decreased from 68.1 degrees for the pure membrane to 38.3 degrees

for membrane number 5 with 5% weight of nanoparticles [18]. In previous studies, a combination of iron oxide with another substance has been used to modify polyethersulfone membranes through the phase inversion method. Bio-inspired iron(III)-dopamine nanoparticles have only been used in gas separation membranes. Therefore, the use of biocompatible dopamine iron nanoparticles in the nanofiltration process and modification of polyethersulfone membranes has not yet been investigated.

In this study, we aim to investigate the effects of using bio-inspired iron(III)-dopamine nanoparticles on the performance of polyethersulfone membranes. However, due to the tendency of iron and dopamine to adhere, there may be a reduction in flux, but it is expected that we will see improvements in anti-fouling properties.

2. Experimental

2.1. Materials

This article aims to investigate the performance of polyethersulfone membranes in nanofiltration by incorporating bio-inspired iron(III)-dopamine nanoparticles as an additive to the membrane base. The phase inversion method was used to construct the membranes, and the modification process is explained in detail below. The membrane base polymer was polyethersulfone with a molecular weight of 58,000 g/mol, while polyvinylpyrrolidone with a molecular weight of 25,000 g/mol was used as a pore-forming agent, and dimethylacetamide with a molecular weight of 87.12 g/mol was used as a solvent. All chemicals composed of Dimethylacetamide (DMAC Mw: 87.12, 0.94 g/cm^3**)** as a solvent, Dopamine (99.95%) and $FeCl_3$ were purchased from Merck. were prepared from Merck. Deionized water was used as a non-solvent in all experiments. Iron salt and dopamine were used to create nanoparticles as additives to the membrane base polymer. A sodium sulfate (Na_2SO_4) solution with a concentration of 1000 mg/L was used as a feed solution. All experiments were conducted at room temperature with a constant salt concentration, and the effect of different nanoparticle concentrations on membrane performance was examined. The chemical structures of these materials are shown in Table 1.

Table 1. Chemical structure of substances

Substance	Abbreviation	structure
Polyether sulfone	**PES**	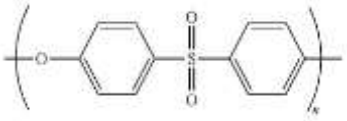
Polyvinyl pyrrolidone	**PVP**	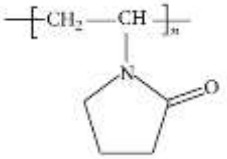
Dimethylacetamide	**DMAC**	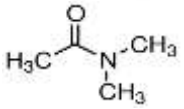
Iron(III) chloride	**$FeCl_3$**	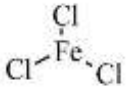
Dopamine	**DA**	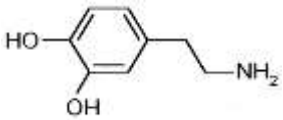

2.2. Synthesis of Nanoparticles

Dopamine, with hydroxyl and amino groups on its six-membered ring, is a suitable compound for attaching to the surface of nanoparticles. The attachment between nanoparticles and dopamine can be achieved by creating hydrogen bonds between hydroxyl groups and the nanoparticle. The functionalization of nanoparticles with dopamine directly deactivates the active hydroxyl groups in non-electrochemical methods by creating hydrogen bonds. Another attachment can be through the Schiff base reaction between the amino group attached to the dopamine ring and aldehyde compounds attached to the nanoparticle. In this work, nanoparticles with a ratio of one-sixth iron to dopamine were synthesized, in which 0.2 g of iron salt and 1.0 g of dopamine were separately mixed with 15 mL of distilled water in a glass container and stirred for approximately 20 minutes on a stirrer. Then, the materials inside the glass containers were mixed together under nitrogen gas to reduce the iron oxidation property, followed by stirring for three hours. After this step, the materials were left in an oven for 24 hours at 50°C to dry. The amount of materials used and the ratio of iron and dopamine were determined experimentally.

2.3. Construction of Membranes

In this study, membranes were synthesized using the phase inversion method with immersion in a non-solvent bath. As shown in Table 1, the polymer, polyether sulfone, does not contain any specific functional groups that can impart unique properties such as high-water affinity or other properties in the membranes made from this polymer. However, this polymer can be used as an agent for membrane synthesis and through it, different membranes can be made using various methods and appropriate modifications can be made to improve membrane performance. Only some polar solvents such as dimethylacetamide exist that can dissolve polyether sulfone. On the other hand, this solvent has sufficient water miscibility, which is essential in the phase inversion process. Therefore, to prepare a polymer solution, polyether sulfone was dissolved in dimethylacetamide solvent and polyvinylpyrrolidone was added as a pore-forming agent. In order to modify the membrane, dopamine iron nanoparticles were added to the polymer solution at different concentrations. The composition of these solutions is given in Table 2.

Table 2. The proportion of polymer solution components (weight percent)

Membrane NO.	Base polymer (polyethersulfone)	Cavity forming polymer (polyvinyl pyrrolidone)	Nanoparticles (iron dopamine)	Solvent (dimethylacetamide)
1	18	1	0	81
2	18	1	0.05	80.95
3	18	1	0.1	80.90
4	18	1	0.5	80.50
5	18	1	1	80

Glassware containing a polymer solution was placed on a magnetic stirrer at a speed of 700 rpm for 6 hours. This resulted in a uniform polymer solution. To ensure even distribution of nanoparticles in the polymer solution and prevent their aggregation in the membrane structure, as well as to remove dissolved bubbles in the solutions, the glassware containing the polymer solution was placed in an ultrasonic device at 20°C for 45 minutes. It is expected that, following the aforementioned steps, the obtained polymer solution is free of air bubbles and the nanoparticles are uniformly dispersed in it. In this stage of the experiment, five membrane samples were prepared, all of which used polyvinylpyrrolidone as a constant additive in membrane preparation. To modify the initial membrane, dopamine iron nanoparticles were used in four different combinations at varying percentages. Subsequently, the polymer solutions were spread on clean and smooth glass slides using a stainless-steel applicator with a thickness of 300 micrometers, creating a thin layer that was immediately immersed in a non-ionic water bath. At this stage, the exchange between solvent and non-solvent resulted in membrane formation. After phase separation and complete membrane formation, the membranes were placed in non-ionic water for 24 hours to extract any remaining solvent and dissolved materials and complete the phase separation process. Afterwards, the membranes were placed between two smooth papers for

24 hours to fully dry. Following these steps, the prepared membranes were ready for testing. Fig. 1 illustrates the membrane casting process.

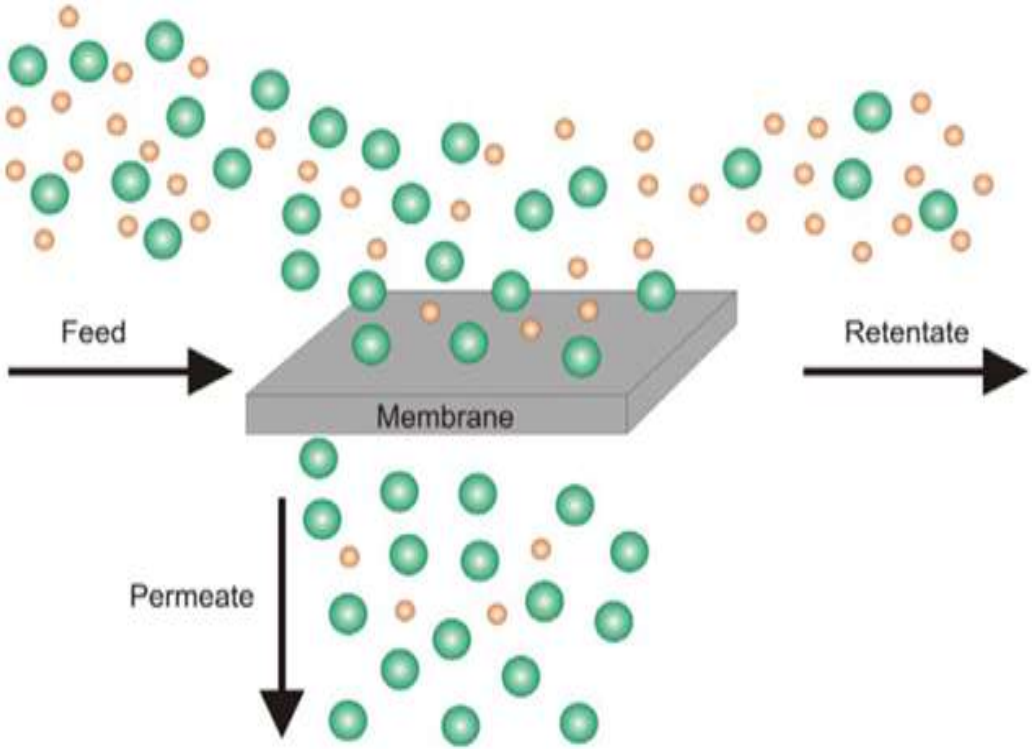

Fig. 1. Membrane casting process

2.4. Characterization

The Fourier transform infrared spectroscopy (FTIR) with a Bruker spectrometer (TENSOR 27), Field emission scanning electron microscopy (FESEM) (MAIA3 model with accelerating voltage of 50 eV), X-ray diffraction (XRD) was applied to characterization membrane. Moreover, 3D surface image provided using optical microscopy along with SPIP software (version 6.4) in the area of 7.5 µm × 10 µm to study the surface roughness of prepared membranes.

2.5. Test Set-Up

Laboratory synthesized membranes, whose fabrication process has been described, were tested in room temperature using a 5/4 cm diameter nanofiltration cell with an effective membrane area of 94/11 cm^2. Nitrogen gas with a purity higher than 99% was used to create pressure driving force on both sides of the membrane. All experiments were conducted at an operational pressure of 5/4 bar. It is worth mentioning that an electric mixer with variable speed of 150-450 rpm was employed in order to minimize the effect of concentration polarization on the membrane surface. The schematic of the closed-end nanofiltration system is illustrated in Fig. 2.

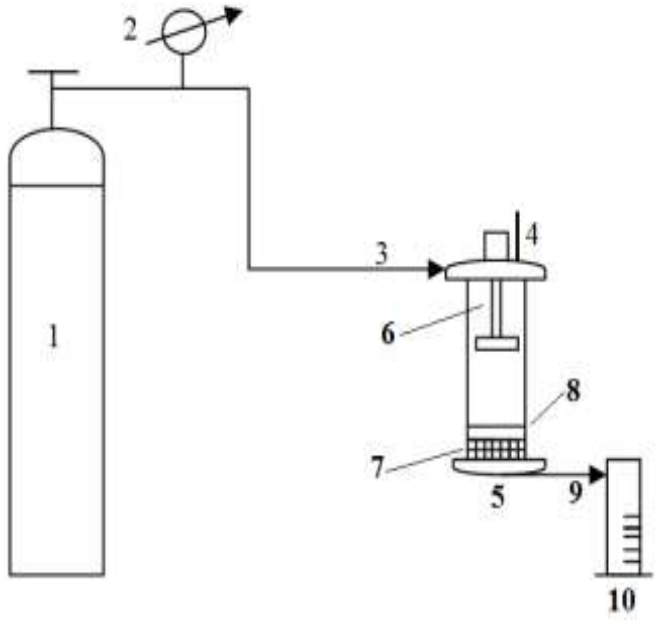

Fig. 2. Closed-end nanofiltration membrane system. (1) Nitrogen gas cylinder
(2) Pressure gauge
(3) Nitrogen inlet to nanofiltration cell
(4) Nitrogen discharge outlet
(5) Nanofiltration cell
(6) Electric stirrer
(7) Membrane filter support
(8) Nanofiltration.

3. Results & Discussion

3.1. Results of Infrared spectrometry

Various tests were conducted to investigate the properties of the membrane after the addition of iron-dopamine nanoparticles. To confirm the presence of these nanoparticles in the membrane structure, an FTIR test was conducted prior to the tests. The results of the FTIR test, as shown in Fig. 3-a, indicated a peak in the range of 18,592 cm^{-1} which corresponds to the Fe-O bond stretching vibrations. A broad absorption in the region of 04,3151 cm^{-1} to 48,3345 cm-1 corresponds to the OH group stretching vibrations and the N-H group stretching vibrations. The peak at 1500 cm-1 corresponds to the N-H bond bending vibration. Peaks at 36,1285cm-1 and 59,1080 cm-1 also indicate the presence of the C-N bond vibrations in dopamine. The appearance of a peak at 78,1600 cm-1 in the IR spectrum, which is attributed to the double bond C=C in dopamine, can be the reason for the connection of dopamine to iron nanoparticles. In Fig. (3b, 3c), a comparison was made between the infrared spectra of the modified membrane and the pure polyethersulfone (PES) membrane. The structure of dopamine, as evidenced by the N-H and C=C bonds, affected the absorption peaks in the region of 1500-1600 cm^{-1}. These peaks were shorter in the modified membrane compared to the pure PES membrane. Furthermore, the peak associated with the C-H bond vibration was observed at 3096 and 3069 cm^{-1}. The bands at 3628 and 3553 cm^{-1} were attributed to the stretching vibration of the OH bond. The peaks related to the aromatic rings of PES were observed at 835 and 1010 cm^{-1}. The peak at 1293 cm^{-1} was characteristic of the stretching vibration of the sulfone group (O=S=O), while the peak at 1253 cm^{-1} represented the C-O-C stretching vibration in PES. Finally, the peak at 1147 cm^{-1} corresponded to the stretching vibration of the N-C bond in the structure of iron-dopamine nanoparticles, providing evidence for their presence in the membrane structure [20-22].

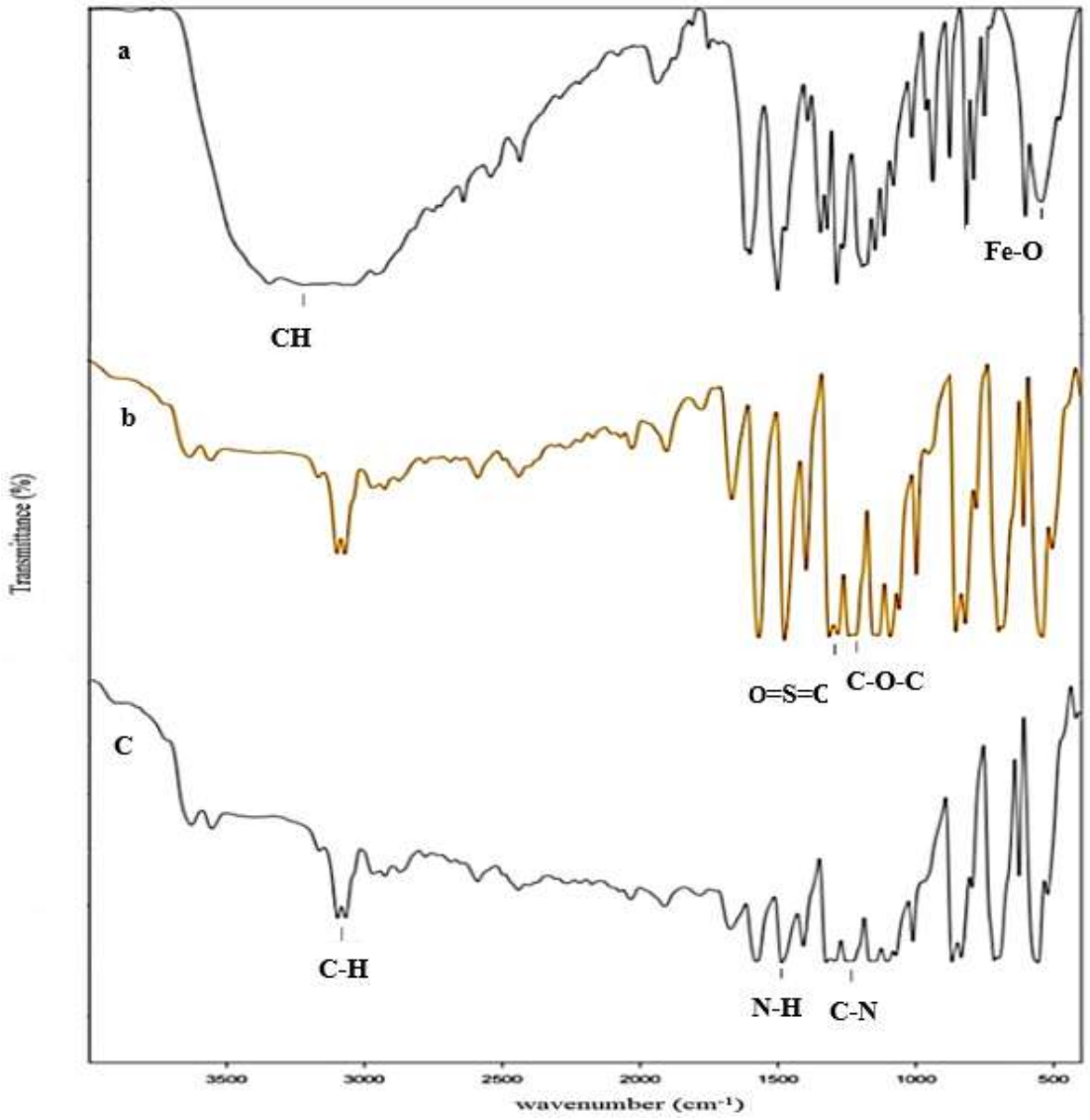

Fig. 3. The results of FTIR test (a) iron dopamine nanoparticles (b) pure membrane, (c) modified membrane with one weight percent of iron dopamine nanoparticles.

3.2. Results of X-ray Diffraction for Nanoparticles

Based on Fig. 4, the structure of dopamine coated iron nanoparticles was studied using X-ray diffraction (XRD), a common method for characterizing crystalline materials. In this graph, the position of the peak is defined as a function of the angle θ2. The sharp and intense peaks indicate the crystallinity of the nanoparticles and were in accordance with the peaks of dopamine and iron samples obtained from literature sources. The average size of the crystals can be calculated from the Scherrer equation (1) based on the XRD data of the sample [23].

$$D = \frac{k\lambda}{\beta \cos\theta} \quad (1)$$

In this regard, D is the dimensions of the crystal (in nanometers), K is a constant value (approximately 9/0), λ is the wavelength of the incident radiation (whose value is 154/0 nanometers, given that the radiation is from the Ka line of copper), β is the bandwidth at half maximum peak (which should be converted to unit of length in degrees), and the scattering angle (θ) are considered to determine the size of the nano iron-dopamine particles.

$$D=\frac{0.94\times0.154}{\frac{3.1415\times0.1476}{180}\times cos(16.77)}=60.31\ nm \quad (2)$$

As can be seen from the above calculations, the size of the crystals was found to be 31.60 nanometers.

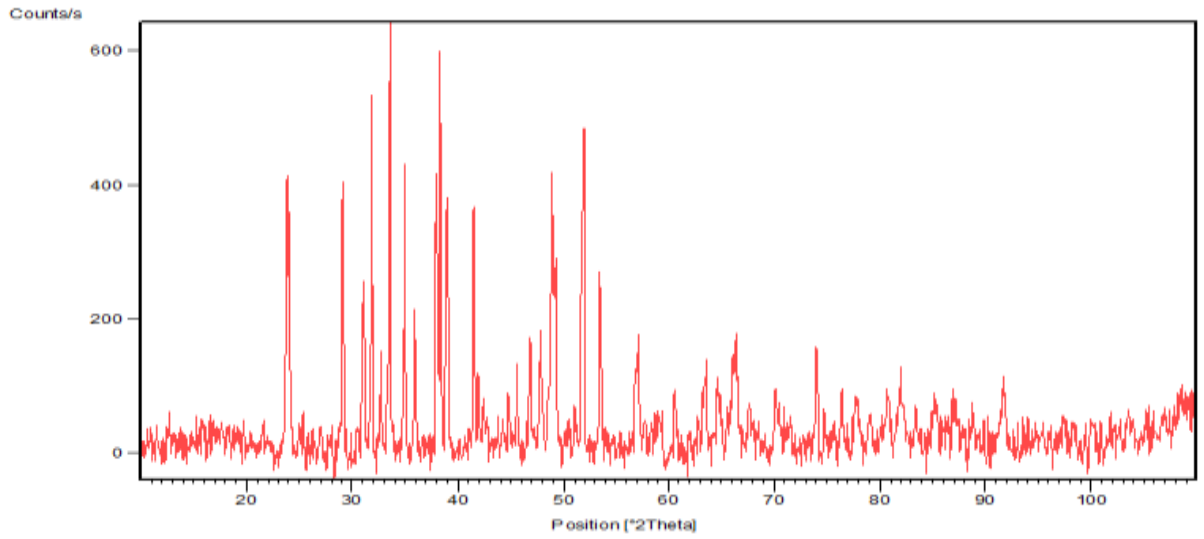

Fig. 4. XRD diagram of iron dopamine nanoparticles

3.3. FESEM/EDS and mapping study

The most appropriate method for investigating the structure and morphology of membranes is through the use of a scanning electron microscope, or FESEM. Fig. 5 shows electron microscope images taken from cross-sections of membranes made using different concentrations of dopamine-coated iron nanoparticles in a polymeric solution prepared by the phase change method. All images are provided on a 10-micron scale. As shown in Figure 4, all of the membranes have an irregular structure with a dense separating layer and tubular cavities in the support layer. The dopamine-coated iron nanoparticles contain oxygen in their structure. This causes a decrease in the phase separation time during membrane formation in the water bath. Therefore, adding them to the membrane structure increases the phase separation rate, which leads to the formation of porous and thin layer at the top of the membrane. As can be seen in the images, adding dopamine-coated iron nanoparticles to the polymeric solution results in a denser separating layer, increased porosity in the support layer, and the formation of large and finger-like cavities in the membrane structure [24-26]. In Fig. 5, it can be observed that as the percentage of nanoparticles in the membrane increases, the structure within the membrane becomes more disordered and asymmetric, resulting in an easily observable increase in its porosity. At a weight percentage of 1.0%, the introduction of dopamine-coated iron nanoparticles in membrane 3 results in a higher porosity that readily facilitates permeation between the solvent (DMAc) and nonsolvent (water) during phase inversion. However, with the addition of more nanoparticles in membranes 4 and 5, the average pore size and porosity decrease, which may be attributed to the clogging of pore openings by nanoparticles that have become adhesive. In the modified membrane with 5.0% weight nanoparticles, depicted in Fig. 5, it is evident how the nanoparticles themselves can cause pore clogging and a reduction in flow. Nonetheless, it should be noted that the primary function of separation by the membrane lies with its top, dense separation layer, and an increase in pore size and porosity in the lower layer does not influence membrane separation, but only serves to decrease the mechanical strength of the membrane [27].

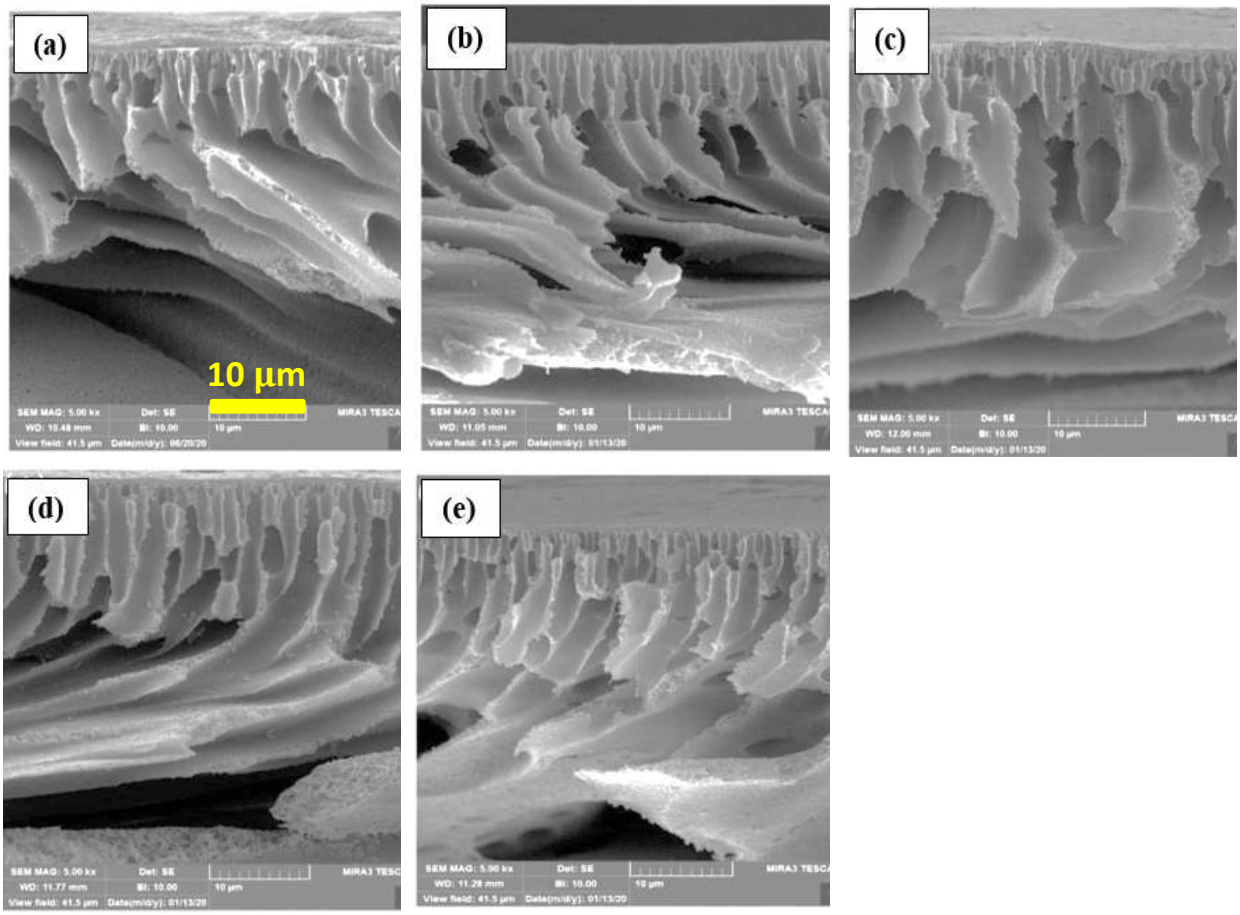

Fig. 5. SEM images of the cross section of the fabricated membranes. (a) Membrane without nanoparticles, (b) Membrane containing 0.05% by weight of iron dopamine nanoparticles, (c) Membrane containing 0.1% by weight of iron dopamine nanoparticles, (d) Membrane containing 0.5% by weight of iron dopamine nanoparticles, (e) Membrane containing 1 Dopamine iron nanoparticle weight percentage.

From membrane sample number 3 with 0.1% by weight of iron dopamine nanoparticles, IDEX analysis was taken to determine the components inside the membrane, the results of which are given in Table 3.

Table 3. The weight percentage of the components in the membrane with 0.1 weight percent of iron dopamine nanoparticles, the result of EDS analysis

Element	Carbon (C)	Oxygen (O)	Ferrum (Fe)	Total
Weight Percent	46.71	46.19	7.10	100.00

In Fig. 6, an energy spectrum graph is shown showing the main peaks for a membrane with 1.0 wt% of iron-dopamine nanoparticles. Peaks corresponding to oxygen and iron are indicated, confirming the presence of these elements in the membrane. The number of X-rays in each peak is proportional to the number of atoms, and the intensity of each peak can be used to determine the concentration of each element in the sample. Each element emits a unique X-ray spectrum that is characteristic to that element.

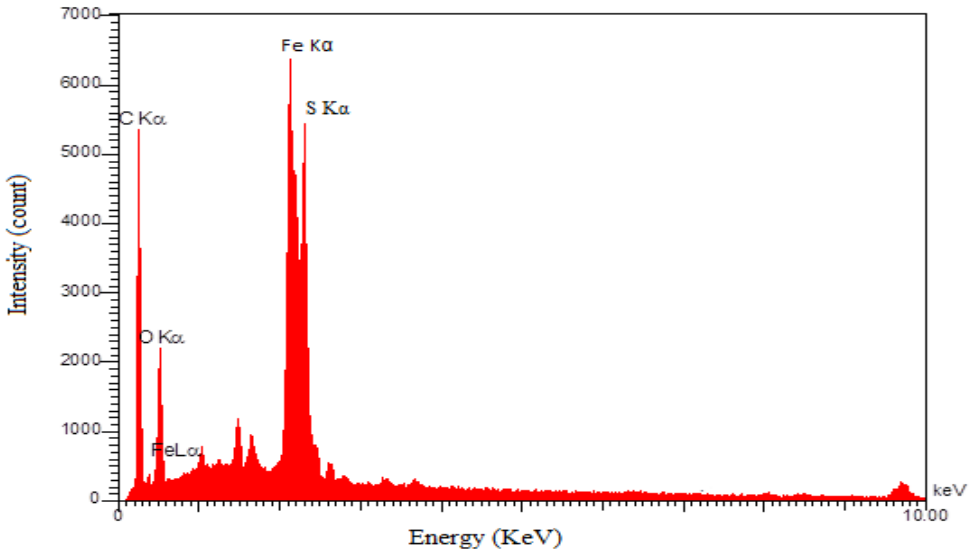

Fig. 6. The diagram of the measured energy spectrum and the main peaks for the membrane with 0.1% by weight of iron dopamine nanoparticles.

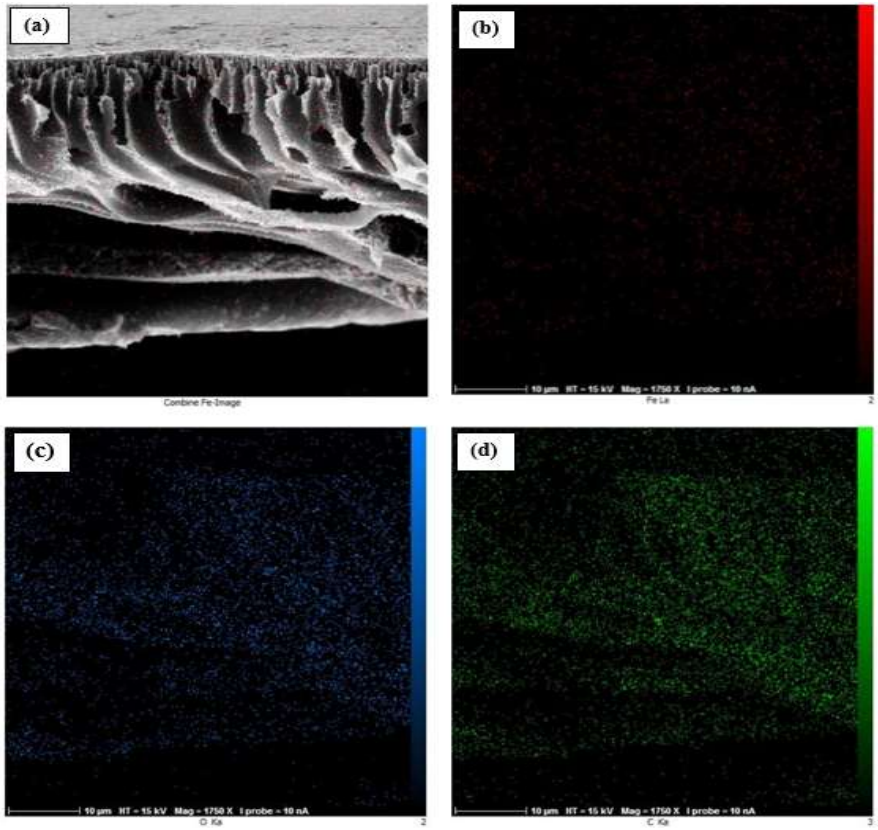

Fig. 7. EDX point analysis: (a) distribution of iron element dispersion in the cross-sectional photo of the scanning electron microscope of the membrane with 0.1% by weight of iron dopamine nanoparticles, (b) point mapping of the iron element in the membrane structure with 0.1% by weight of iron dopamine nanoparticles (c) point mapping of the oxygen element in the membrane structure with 0.1% by weight of iron dopamine nanoparticles, d) point mapping of the carbon element in the membrane structure with 0.1% by weight of iron dopamine nanoparticles.

To investigate the formation and dispersion of nanoparticles on the membrane surface, field-emission scanning electron microscopy images have also been used. In Fig. 8, we see that nanoparticles with a spherical structure and diameters ranging from 25 to 45 nm have been formed. The reason for the mismatch with the crystal sizes calculated from the Scherrer equation is the aggregation and adhesion of the particles. Figure 7a shows iron-dopamine nanoparticles at a scale of 200 nm, and Fig. 8b shows the surface of the membrane with 1 wt% of iron-dopamine nanoparticles, where the density of the nanoparticles is visible due to the high concentration used in the sample.

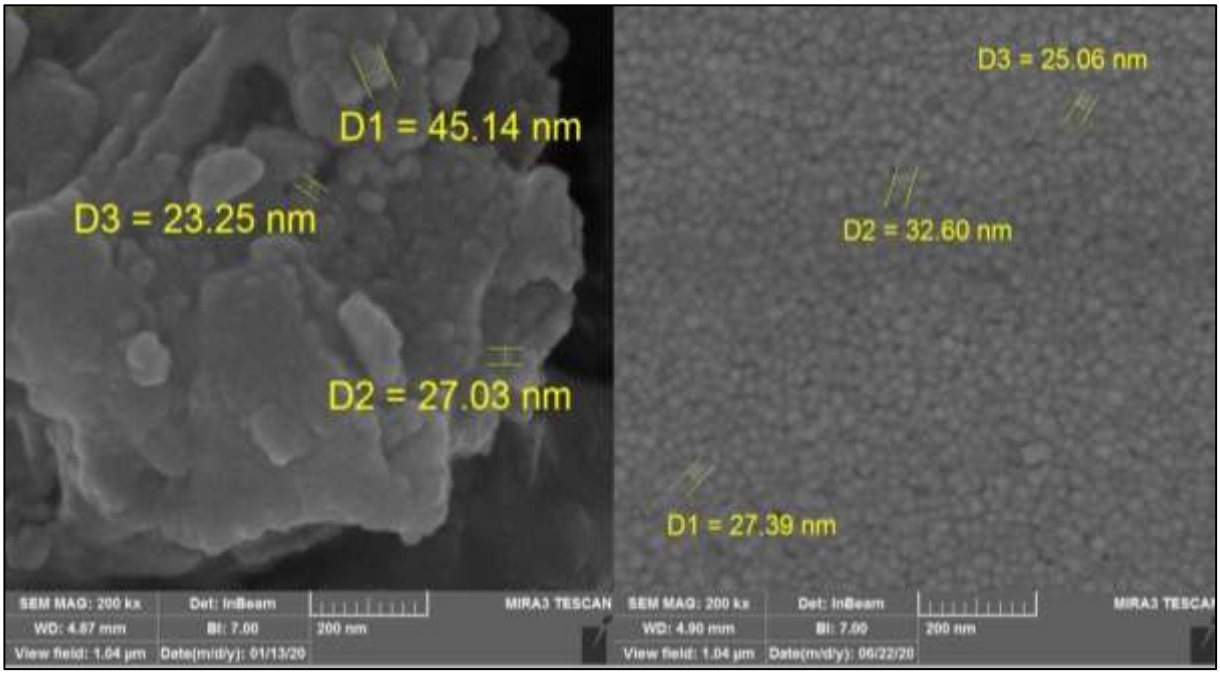

Fig. 8. SEM images of (a) image of iron dopamine nanoparticles on a scale of 200 nm, (b) image of the surface of the membrane with 1% by weight of iron dopamine nanoparticles on a scale of 200 nm.

Fig. 9 illustrates the changes in membrane porosity caused by the addition of nanoparticles to a polymer solution. As the number of nanoparticles increases in the polymer solution, the water affinity also increases. With the increase in nanoparticles in the polymer solution, the viscosity of the solution also increases, resulting in a decreased exchange rate and therefore a reduction in porosity. One can justify the increase in porosity by the low viscosity of the initial polymer solution, where water affinity dominates over viscosity, resulting in increased porosity [28].

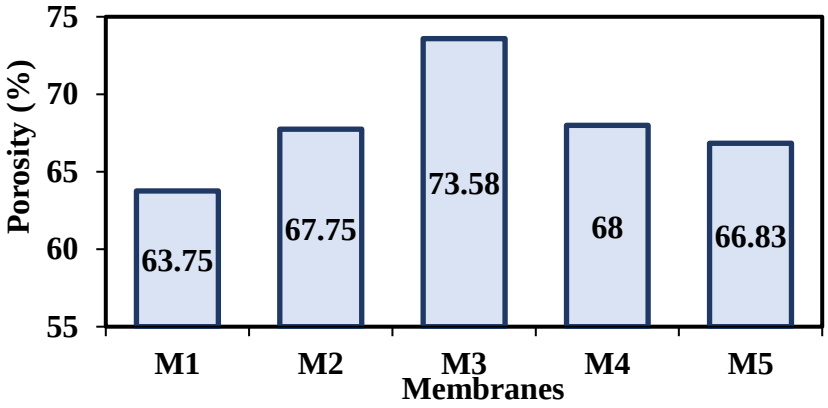

Fig. 9. The effect of iron dopamine nanoparticles on the porosity of fabricated membranes

3.4. Results of Contact Angle

Measuring the contact angle of water is a tool used to evaluate the wettability of a membrane surface. Generally speaking, a lower contact angle indicates a higher degree of wettability, which can improve the membrane's anti-fouling properties. Surface roughness, particle heterogeneity, and particle shape are among the factors that can influence the contact angle measurement. Fig. 10 demonstrates the results of contact angle measurements where adding nanoparticles reduced the contact angle. Moreover, polyethersulfone, which is hydrophobic in nature, had its hydrophobicity reduced upon nanoparticle addition. The lowest contact angle was observed on membrane number 5 with the highest percentage of nanoparticles by weight (1%), indicating a greater degree of wettability. However, this increased wettability did not lead to improved membrane flux, possibly due to nanoparticle agglomeration at higher concentrations.

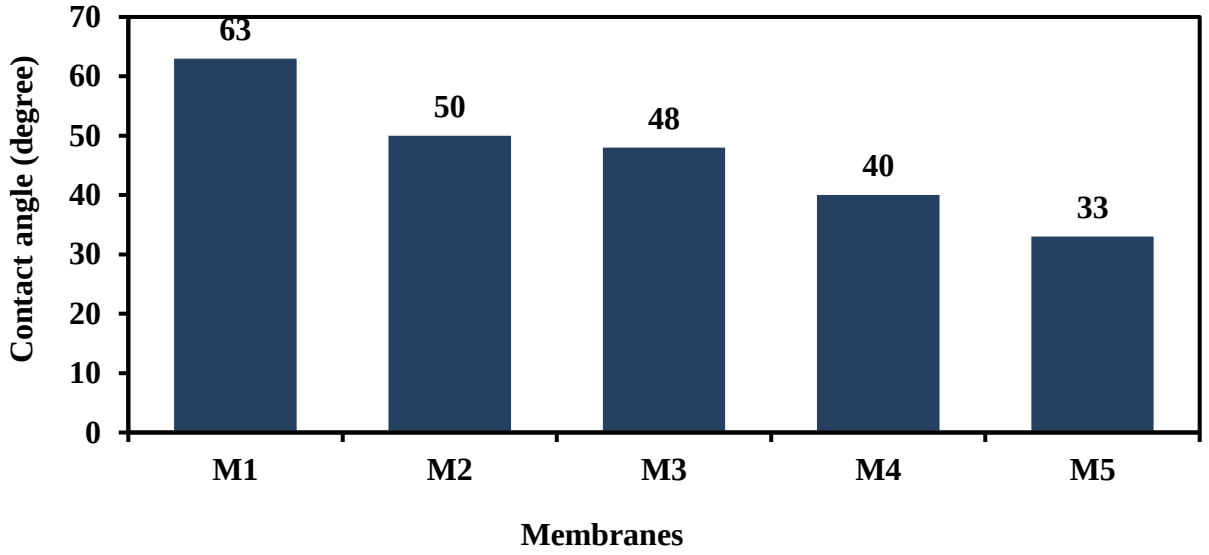

Fig. 10. The effect of iron dopamine nanoparticle concentration on water contact angle of fabricated membranes

3.5. Investigating pure water flux and average surface pore size

The results of pure water flux across the membrane are shown in Figure 10. There are many factors that affect the flux of water through the membrane, including water affinity, porosity, morphology, and pore size. As observed, with an increase in the concentration of nanoparticles, the changes in the flux of pure water passing through the membrane are almost downward. The pure water flux passing through all samples is less than that of the sample without nanoparticles. This phenomenon can be explained by the filling of the surface cavities of the membrane by nanoparticles, which in turn reduces the size and capacity of membrane cavities for water molecules to pass through. The decrease in pure water flux in membrane number 2 can also be explained by a decrease in the size of surface cavities, as the small number of nanoparticles did not cause any change in membrane affinity and only filled the surface cavities.

In membrane number 3, an increase in porosity is expected to result in an increase in pure water flux. However, as shown in the field-emission scanning electron microscopy Fig. 5, the membrane has become more porous, but the channels created are blocked due to particle agglomeration.

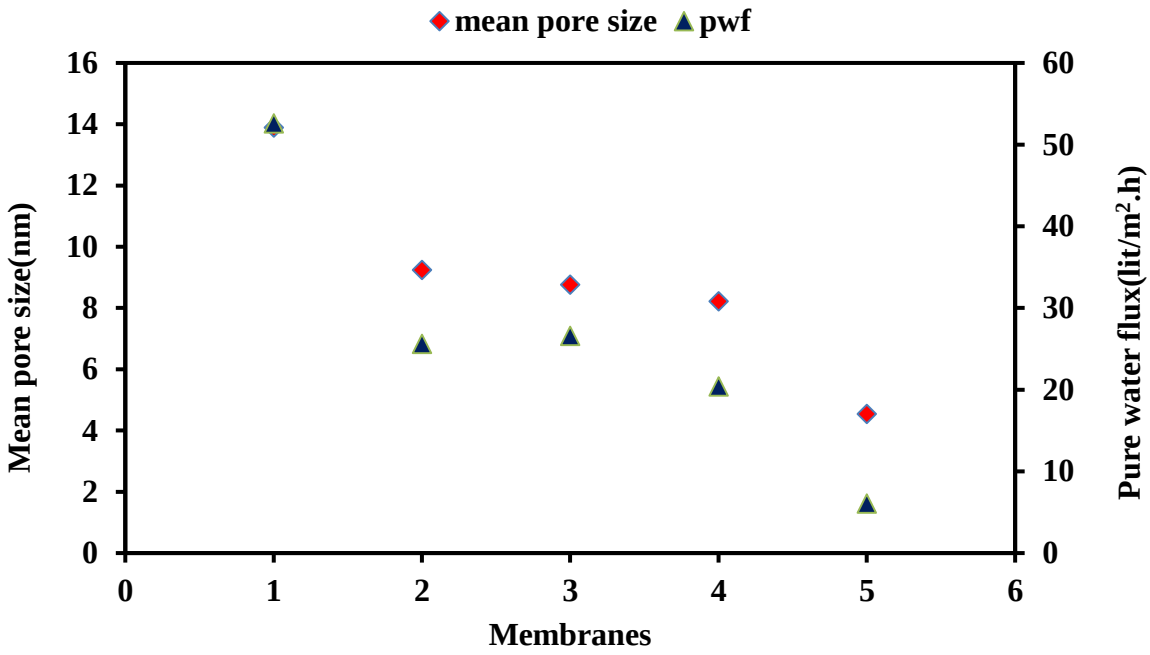

Fig. 11. Effect of iron dopamine nanoparticles on pure water flux and pore size of fabricated membranes

3.6. Membrane separation performance

Permeability and selectivity are two important factors in determining the performance of a membrane. The presence of nanoparticles in a polymer solution results in changes in the permeation flux and membrane reversibility, leading to performance enhancement at suitable concentrations. The permeation flux of the membranes was measured at a pressure of 4.5 psi, and the results of salt permeation and rejection fluxes are presented in Fig. 11. Initially, a decrease in flux is observed for membrane 2 due to a noticeable reduction in particle size from 13.9 nm to 9.2 nm, as observed in Fig. 12. Subsequently, the permeation flux increases from 28.03 to 33.71 and then begins to decrease again. In fact, water compatibility and membrane structure are two important factors that affect flux and separation from the membrane, and the separation mechanism in filtration is based on the size exclusion of pores. In this regard, membrane 3 with a weight percentage of 1.0% of nanoparticles, which has the highest porosity, had a slight increase in flux, which then decreased with an increase in nanoparticles.

Over time during a separation process, a reduction in the permeate flux of a membrane is anticipated. The main reason for this reduction is the occupation of surface voids and membrane structure by accumulated and unpassed particles, leading to the formation of a resistance layer against mass transfer and occurrence of concentration polarization near the membrane surface. This leads to a decrease in water uptake on the membrane surface, resulting in reduced flux. The selectivity of solutes in water by a nanofiltration membrane varies depending on particle size, electrostatic repulsion force, and adsorption levels of different particles onto the membrane surface, which rely upon the membrane surface properties, particles in the solution, and operating conditions. It is observed that an increase in nanoparticle concentration leads to an increase in salt rejection. For example, in Sample 5, a decrease in rejection is expected because of the existing fouling, but the tests performed have shown an increase in rejection. This increase in rejection can be explained by the dominance of the hydrophilicity property of the particles. The contact angle of water droplets with the membrane surface also supports this claim.

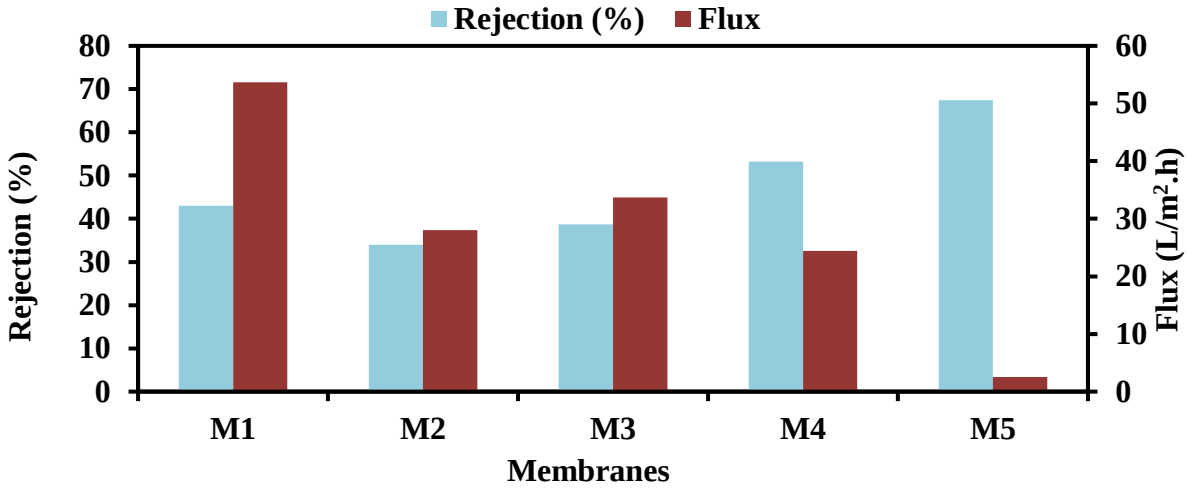

Fig. 12. The effect of adding iron dopamine nanoparticles on the amount of rejection and flux of prepared membrane

3.7. Water Content

The content of the membrane is an indicator of its water affinity, moisture absorption, swelling, and degree of porosity [29]. The effect of iron-dopamine nanoparticles concentrations on the prepared membranes water content is shown in Fig. 13. As shown in the figure, initially, by increasing the concentration of iron-dopamine nanoparticles in the polymer solution, the content of the membrane's water increases. Generally, it is accepted that increasing the exchange rate between water and the solvent can create a membrane with higher porosity and vice versa [28]. In membrane 2 with a 0.5% weight fraction of nanoparticles, we observe an increase in water content due to increased porosity. However, after that, by adding more nanoparticles, the water content decreases, which could be attributed to the reduction in pore size, decrease in porosity, increased viscosity of the solution, and accumulation of nanoparticles in the empty spaces, resulting in the inability to store water. Clogging of the pores during phase separation could also be another reason for the decrease in water content due to the movement of nanoparticles towards the membrane surface.

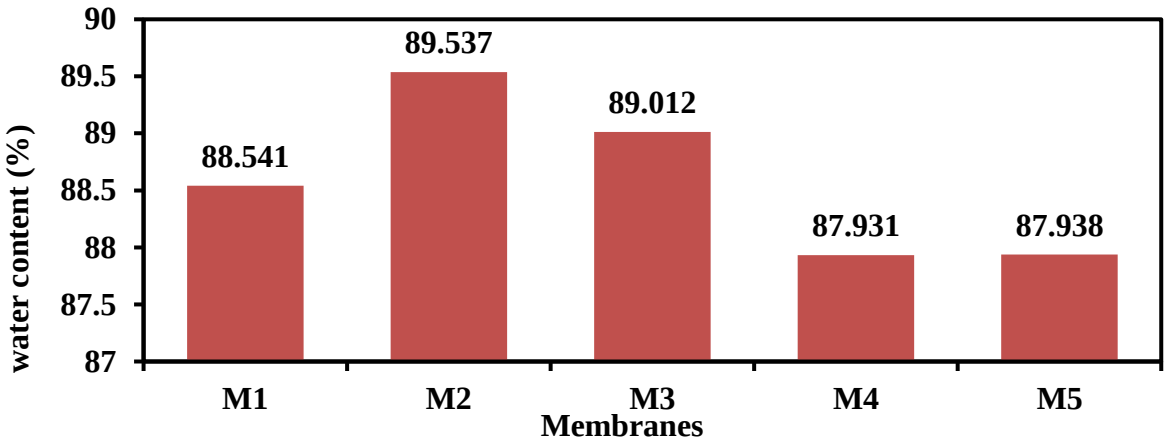

Fig. 13. The effect of the concentration of iron dopamine nanoparticles on the water content of the constructed membranes

The water content of the membrane indicates its water affinity, moisture absorption, swelling capacity, and degree of porosity. Fig. 13 illustrates the effect of varying concentrations of iron-dopamine nanoparticles on the water content

of the fabricated membranes. Initially, with an increase in nanoparticle concentration, the water content rises. This can be attributed to the hydrophilic nature of the nanoparticles, which promotes water retention within the membrane structure. Moreover, the nanoparticles facilitate an increased exchange rate between water and the solvent during phase separation, leading to the formation of membranes with higher porosity and water uptake. However, at higher nanoparticle concentrations, the water content begins to decline. This decrease is likely due to the aggregation of nanoparticles, which reduces the effective pore size and porosity of the membrane. Additionally, the increased viscosity of the polymer solution at higher nanoparticle concentrations can hinder the solvent-nonsolvent exchange during phase inversion, further reducing porosity and water retention. The movement of nanoparticles toward the membrane surface during phase separation may also contribute to pore clogging, preventing the membrane from storing water effectively. These findings underscore the dual role of nanoparticles: while they initially enhance hydrophilicity and porosity, excessive concentrations lead to aggregation and reduced performance. This balance is crucial in optimizing the membrane properties for desired applications.

3..8. Membrane surface Morphology

In order to examine the surface roughness of the membrane, three-dimensional images were used as shown in Fig. 14. Consistent with the figure, sharp irregularities are observed on the surface of the membrane without nanoparticles, indicating the inherent hydrophobicity of the polyethersulfone. According to Table 4, which displays roughness parameters, after the addition of iron dopamine nanoparticles to the membrane structure, the level of roughness or hardness of the membrane surface slightly increased which may be attributed to the presence of nanoparticles on the surface and the creation of more pores during the phase change process. A rough surface membrane has a greater ability to trap and absorb ions on its surface, and increasing the concentration of ions on the surface creates a driving force of concentration difference that increases ion transfer from inside the membrane and decreases membrane flux. Surface roughness is a critical factor in determining membrane performance, as it directly influences properties such as ion adsorption, fouling resistance, and permeability. The three key roughness parameters—average roughness (Ra), average height of the highest roughness peaks (Rz), and root mean square of roughness (Rq)—were analyzed and are summarized in Table 4. As shown, the incorporation of iron-dopamine nanoparticles significantly alters the membrane's surface roughness. The Ra, Rz, and Rq values increased with the addition of nanoparticles up to a concentration of 1.0 wt%, indicating the formation of a more irregular and textured surface. This increased roughness can enhance ion adsorption due to the larger surface area available for interaction. For example, a rougher surface promotes greater trapping of ions and particles, creating a concentration gradient that facilitates ion transfer across the membrane. However, excessive roughness, as observed in membrane M5, can also lead to undesirable effects such as increased fouling. A highly textured surface may provide more sites for protein or particle adhesion, which can block the pores and reduce water flux. This is evident from the flux reduction observed in membrane M5 (Fig. 12), where nanoparticle aggregation contributed to pore clogging and surface irregularities. The optimal membrane, M3, exhibits a balance between roughness and performance. Its moderate roughness (Ra = 334.3 nm) provides sufficient surface area for ion adsorption without significantly increasing fouling risks. This balance highlights the importance of optimizing roughness parameters to achieve high separation efficiency and anti-fouling properties in nanofiltration membranes. This flux reduction for membrane number 5 with 1% weight of iron dopamine nanoparticles in Fig. 12 is visible.

Table 4. Surface roughness parameter values

Membrane NO.	Average surface roughness (Ra, nm)	The average of the highest roughness heights (Rz, nm)	root mean square (Rq, nm)
M1	504.1	217.3	88.1
M2	863.2	96.3	621.3
M3	334.3	342.4	419.4
M4	124.4	78.6	236.5
M5	783.4	722.9	7.6

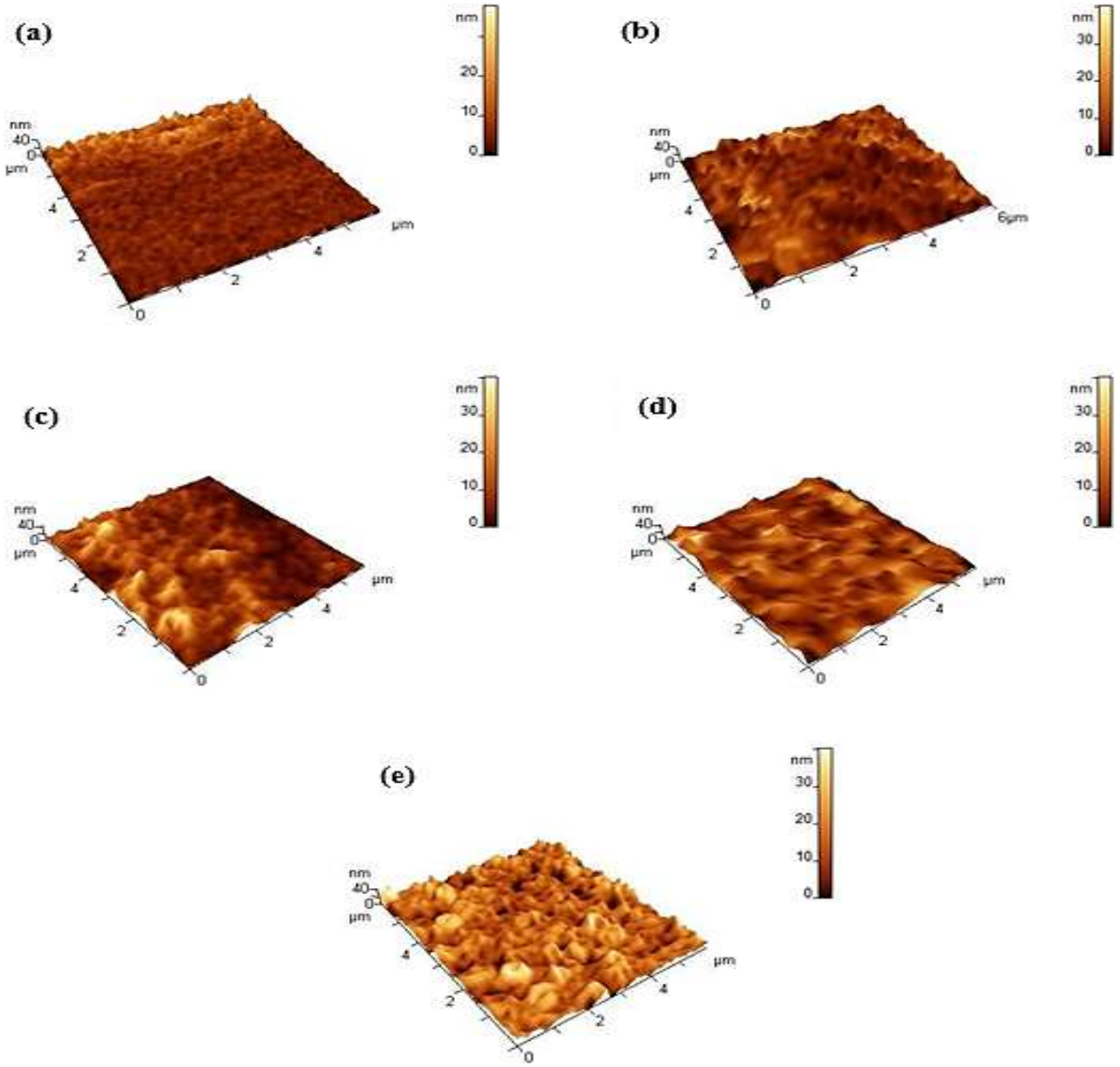

Figure 1. 3D surface images: a) pure polyether sulfone membrane, b) membrane containing 0.05% by weight of iron dopamine nanoparticles, c) membrane containing 0.1% by weight of iron dopamine nanoparticles, d) membrane containing 0.5% by weight of iron dopamine nanoparticles, e) membrane Contains 1% by weight of iron dopamine nanoparticles.

3.8. Examination of agglomeration parameters

The amount of permeate flow through the membrane for pure water before and after the separation of the milk solution was calculated, as well as the permeate flow of the milk and water solution. These values are shown in Fig.14. As the figure indicates, the overall fouling rate decreased irreversibly after adding a small amount of nanoscale particles. However, after adding 1.0 weight percent of dopamine-coated iron nanoparticles, these parameters increased. The higher reversible fouling rate implies better detachment of the captured particles from the membrane surface during the cleaning process. The fouling behavior of the membranes, characterized by reversible and irreversible fouling rates, provides critical insights into their performance. The observed trends can be attributed to the role of nanoparticle dispersion and agglomeration within the membrane structure. At lower nanoparticle

concentrations, such as 0.5 wt%, the particles are more uniformly dispersed, resulting in smoother surfaces with fewer irregularities. This uniformity enhances the detachment of fouling particles during cleaning, leading to a higher reversible fouling rate and improved anti-fouling behavior. However, at higher nanoparticle concentrations (e.g., 1.0 wt%), agglomeration occurs due to the strong interactions among nanoparticles. This aggregation creates surface irregularities and clogs the membrane pores, leading to increased total fouling and a lower reversible fouling rate. The agglomerates trap fouling particles more effectively, making their removal during cleaning more challenging and resulting in a higher irreversible fouling rate. These findings highlight the delicate balance between nanoparticle concentration and membrane performance. Proper dispersion of nanoparticles is crucial for maintaining the anti-fouling properties of the membrane while minimizing irreversible fouling. This underscores the importance of optimizing nanoparticle loading to achieve the desired balance between fouling resistance and membrane efficiency. The lower overall fouling rate, and the greater reversible fouling rate lead to enhance membrane performance. All the nanomodified membranes showed higher reversible fouling rates and lower irreversible fouling rates compared to the neat polyethersulfone membrane. The overall fouling rate increased from 4.87% for neat polyethersulfone to 5.60% for membrane number 3 with 1.0 weight percent nanoparticles, and the irreversible fouling rate decreased from 61.82% in neat polyethersulfone to 3.41% in membrane number 3 with 0.5 weight percent nanoparticles. The most significant difference in the antifouling capability of these membranes is attributed to the irreversible fouling rate. Among the constructed membranes, the highest reversibility adherence belongs to the membrane with 0.5% dopamine-iron weight, which may be due to its smoother surface. As stated, a high surface roughness results in greater protein adhesion to the membrane surface. Addition of 1% weight of nanomaterials in membrane number 5 reduces the reversibility adherence and increases irreversible adherence and total adherence, which is caused by the agglomeration of nanomaterials. A membrane containing 1.0% weight of dopamine-iron exhibits the lowest total adherence and a relatively lower irreversibility adherence, therefore showing better performance in terms of adherence compared to other constructed membranes. It is observed that the surface properties and the structure of nanomaterials play a key role in improving the anti-adhesion properties and performance of the membrane

.

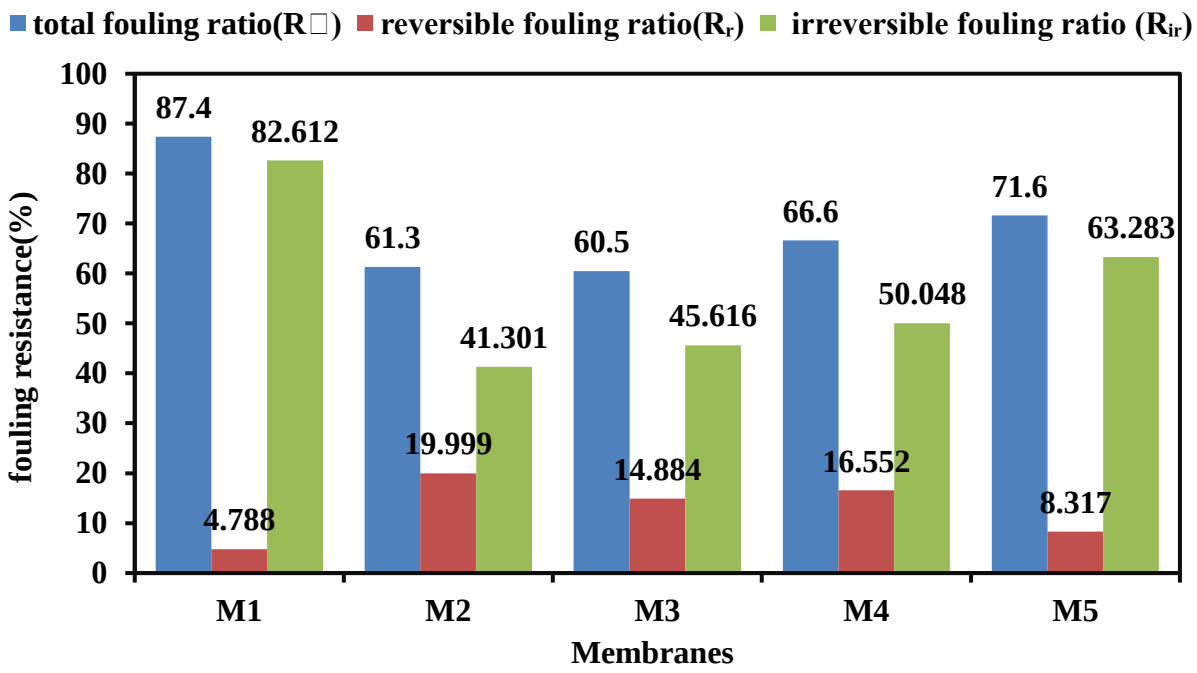

Fig. 15. The effect of total fouling, reversible clogging and irreversible clogging on membranes

3.9. Checking the flow recovery percentage

The most appropriate parameter for comparing and investigating the anti-fouling properties of fabricated membranes is the percentage of flux recovery. As shown in Fig. 16, all modified membranes exhibit higher flux recovery percentages compared to the pure polyethersulfone membrane. However, this trend is not consistent with increasing nanoparticle concentrations. The decrease in flux recovery at higher nanoparticle concentrations may be attributed to the accumulation and agglomeration of nanoparticles, which can reduce their effective surface area and hinder their interaction with the membrane surface. Although increasing nanoparticle concentrations improve the hydrophilicity of the membrane surface, this does not always correlate with improved fouling resistance. The membrane containing 0.1 wt% iron dopamine nanoparticles showed the lowest overall fouling and the highest flux recovery percentage, indicating better performance. However, membranes containing 0.5 and 1 wt% nanoparticles exhibited lower flux recovery percentages, suggesting that higher nanoparticle concentrations do not necessarily result in better anti-fouling behavior. This could be due to the non-uniform dispersion of nanoparticles at higher concentrations, leading to nanoparticle aggregation. The active groups on the nanoparticle surfaces tend to promote aggregation, creating gaps in the membrane's top layer. These gaps can trap proteins, which become difficult to remove during cleaning, thereby reducing the membrane's flux recovery. Consequently, while hydrophilicity increases with higher nanoparticle content, this effect is counteracted by the negative consequences of aggregation and poor dispersion, which lead to reduced membrane performance [30].

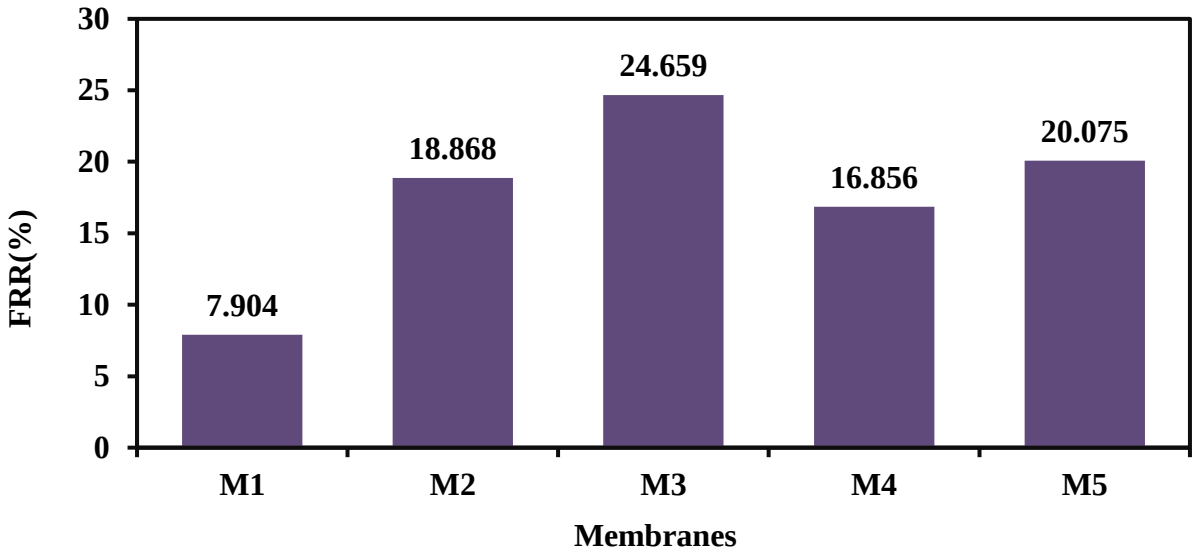

Fig. 16. Flow recovery percentage chart

4. Conclusion

In this study, the modification of polyethersulfone nanofiltration membranes with varying concentrations of iron dopamine nanoparticles was investigated. The membranes were prepared using the phase inversion method and immersion precipitation in a non-solvent bath. Electron microscopy images of cross-sections were obtained to examine the effect of nanoparticle addition on the morphology and structure of the membranes. According to these images, the pore size of the cavities decreased with the addition of iron dopamine nanoparticles to the polymer solution. Additionally, by examining the 3D surface images, it was observed that membrane number 5 was the roughest among all membranes. The porosity of the membranes also increased and then decreased with the addition of nanoparticles until membrane number 3, which was considered as the optimal membrane. This higher density was mostly observed in membrane number 3. The contact angle results of the studied membranes showed that the hydrophilicity of the membrane increased with increasing nanoparticle concentration in the polymer solution. The water content percentage also increased in membrane number 2 with increasing nanoparticle concentration, but then decreased. Water flux also decreased with increasing nanoparticle concentration in the polymer solution, and only slightly increased in membrane

number 3, but overall decreased compared to pure polyethersulfone. Although it was expected that water flux would increase in the optimal membrane due to increased porosity and hydrophilicity, as seen in the field-emission scanning electron microscopy images, most of the channels created in the membrane structure were blocked due to nanoparticle agglomeration, leading to a decrease in porosity and water content for membranes with higher nanoparticle concentrations. Membrane number 3 had the lowest overall fouling rate and a higher percentage of flux recovery compared to other membranes, making it the optimal membrane with a nanoparticle concentration of 1.0 wt%. This study demonstrated that iron dopamine nanoparticles are a suitable option for improving the hydrophilicity, salt rejection, and anti-fouling properties of nanofiltration membranes.

Conflicts of Interest

The authors declare that they have no known competing financial interests or personal relationships that could have appeared to influence the work reported in this paper.

Author information

*Corresponding Author: Fahime Parvizian, Samaneh Bandehali
Email: f-parvizian@araku.ac.ir, s.bandehali@abru.ac.ir

References

[1] J. D. Seader, E. J. Henley, D. K. Roper, Separation process principles. Wiley, New York, Vol. 25 (1998).
[2] E. Drioli, L. Giorno, Comprehensive membrane science and engineering. Newnes, Vol. 1 (2010).
[3] Y. Li, S. Wang, H. Wu, J. Wang, and Z. Jiang, Bioadhesion-inspired polymer–inorganic nanohybrid membranes with enhanced CO_2 capture properties. J. Mater. Chem., 22(37) (2012) 19617–19620. https://doi.org/10.1039/c2jm34347a.
[4] L. Qi, Z. Xu, Lead sorption from aqueous solutions on chitosan nanoparticles. Colloids Surf. A, 251(1-3) (2004) 183–190. https://doi.org/10.1016/j.colsurfa.2004.03.001.
[5] J. Mukherjee, D. Malhotra, S. Gautam, and M. N. Gupta, Green synthesis of nanocomposites consisting of silver and protease alpha chymotrypsin. Ultrason. Sonochem., 20(4) (2013) 1054–1061. https://doi.org/10.1016/j.ultsonch.2012.12.014.
[6] M. F. Ali, S. Abbas, A review of methods for the demetallization of residual fuel oils. Fuel Process. Technol., 87(7) (2006) 573–584. https://doi.org/10.1016/j.fuproc.2006.01.004.
[7] P. Marchetti, M. F. Jimenez Solomon, G. Szekely, and A. G. Livingston, Molecular separation with organic solvent nanofiltration: a critical review. Chem. Rev., 114(21) (2014) 10735–10806. https://doi.org/10.1021/cr500075k.
[8] H. Yacubowicz, J. Yacubowicz, Nanofiltration: properties and uses. Filtr. Sep., 42(7) (2005) 16–21. https://doi.org/10.1080/19443994.2014.943061.
[9] R. R. Sharma, R. Agrawal, S. Chellam, Temperature effects on sieving characteristics of thin-film composite nanofiltration membranes: pore size distributions and transport parameters. J. Membr. Sci., 223(1-2) (2003) 69–87. https://doi.org/10.1016/S0376-7388(03)00233-9.
[10] L. Li, S. Zhang, X. Zhang, Preparation and characterization of poly(piperazineamide) composite nanofiltration membrane by interfacial polymerization of 3,3′,5,5′-biphenyl tetraacyl chloride and piperazine. J. Membr. Sci., 335(1-2) (2009) 133–139. https://doi.org/10.1016/j.memsci.2009.04.043.
[11] H.J. Zwijnenberg, S. M. Dutczak M. E. Boerrigter, M. A. Hempenius, M. W. Luiten-Olieman, N. E. Benes, M. Wessling, and D. Stamatialis, Novel polyethersulfone nanocomposite membrane prepared by PANI/Fe3O4 nanoparticles with enhanced performance for Cu(II) removal from water. J. Membr. Sci., 415 (2012) 250–259. https://doi.org/10.1016/j.memsci.2011.11.039.
[12] S. Zinadini, A. A. Zinatizadeh, M. Rahimi, V. Vatanpour, H. Zangeneh, and M. Beygzadeh, Novel high flux antifouling nanofiltration membranes for dye removal containing carboxymethyl chitosan coated Fe3O4 nanoparticles. Desalination, 349 (2014) 145–154. https://doi.org/10.1016/j.desal.2014.05.012.

[13] J. Kim, Q. Fu, J. M. Scofield, S. E. Kentish, and G. G. Qiao, Ultra-thin film composite mixed matrix membranes incorporating iron (III)–dopamine nanoparticles for CO2 separation. Nanoscale, 8(15) (2016) 8312–8323. https://doi.org/10.1039/C6NR00200B.
[14] E. Bagheripour, A. R. Moghadassi, S. M. Hosseini, and M. Nemati, Fabrication and characterization of novel mixed matrix polyethersulfone nanofiltration membrane modified by iron-nickel oxide nanoparticles. J. Membr. Sci. Res., 2(1) (2016) 14–19. https://doi.org/10.22079/JMSR.2016.22264.
[15] H. Koulivand, A. Shahbazi, V. Vatanpour, Fabrication and characterization of a high-flux and antifouling polyethersulfone membrane for dye removal by embedding Fe_3O_4-MDA nanoparticles. Chem. Eng. Res. Des., 145 (2019) 64–75. https://doi.org/10.1016/j.cherd.2019.03.021.
[16] E. Bagheripour, A. R. Moghadassi, F. Parvizian, S. M. Hosseini, and B. Van der Bruggen, Tailoring the separation performance and fouling reduction of PES based nanofiltration membrane by using a PVA/Fe_3O_4 coating layer. Chem. Eng. Res. Des., 144 (2019) 418–428. https://doi.org/10.1016/j.cherd.2019.03.001.
[17] A. Moghadassi, S. Moradi, S. Bandehali, Fabrication of antifouling mixed matrix NF membranes by embedding sodium citrate surfactant modified-iron oxide nanoparticles. Korean J. Chem. Eng., 37(11) (2020) 1963–1974. https://doi.org/10.1007/s11814-020-0584-1.
[18] S. Ansari, A. Moghadassi, S. M. Hosseini, A new approach to tailoring the separation characteristics of polyethersulfone nanofiltration membranes by 8-hydroxyquinoline functionalized Fe3O4 nanoparticles. Korean J. Chem. Eng., 37(11) (2020) 2011–2019. https://doi.org/10.1007/s11814-020-0590-3.
[19] I.C. Alves, J.R. Santos, D.S. Viégas, E.P. Marques, C.A. Lacerda, L. Zhang, J. Zhanga, and A.L. Marques, Nanoparticles of Fe2O3 and Co3O4 as efficient electrocatalysts for oxygen reduction reaction in acid medium. J. Braz. Chem. Soc., 30(12) (2019) 2681–2691. https://doi.org/10.21577/0103-5053.20190183.
[20] R. A. Zangmeister, T. A. Morris, M. J. Tarlov, Characterization of polydopamine thin films deposited at short times by autoxidation of dopamine. Langmuir, 29(27) (2013) 8619–8628. https://doi.org/10.1021/la4002298.
[21] S. Belfer, R. Fainchtain, Y. Purinson, and O. Kedem, Surface characterization by FTIR-ATR spectroscopy of polyethersulfone membranes-unmodified, modified and protein fouled. J. Membr. Sci., 172(1-2) (2000) 113–124. https://doi.org/10.1016/S0376-7388(00)00324-4.
[22] F. F. Ghiggi, L.D. Pollo, N.S. Cardozo, and I.C. Tessaro, Preparation and characterization of polyethersulfone/N-phthaloyl-chitosan ultrafiltration membrane with antifouling property. Eur. Polym. J., 92 (2017) 61–70. https://doi.org/10.1016/j.eurpolymj.2017.05.032.
[23] A. Monshi, M. R. Foroughi, M. R. Monshi, Modified Scherrer equation to estimate more accurately nano-crystallite size using XRD. World J. Nano Sci. Eng., 2(3) (2012) 154–160. https://doi.org/10.4236/wjnse.2012.23020.
[24] E. Bagheripour, A. Moghadassi, S. M. Hosseini, Preparation of mixed matrix PES-based nanofiltration membrane filled with PANI-co-MWCNT composite nanoparticles. Korean J. Chem. Eng., 33(4) (2016) 1462–1471. https://doi.org/10.1007/s11814-015-0006-9.
[25] S.M. Hosseini, M. Nemati, F. Jeddi, E. Salehi, A.R. Khodabakhshi, and S.S. Madaeni, Fabrication of mixed matrix heterogeneous cation exchange membrane modified by titanium dioxide nanoparticles: Mono/bivalent ionic transport property in desalination. Desalination, 359 (2015) 167–175. https://doi.org/10.1016/j.desal.2014.11.021.
[26] C. Xu, W. Huang, X. Lu, D. Yan, S. Chen, and H. Huang, Preparation of PVDF porous membranes by using PVDF-g-PVP powder as an additive and their antifouling property. Radiat. Phys. Chem., 81(11) (2012) 1763–1769. https://doi.org/10.1016/j.radphyschem.2012.06.017.
[27] S. Madaeni, A. Rahimpour, Effect of type of solvent and non-solvents on morphology and performance of polysulfone and polyethersulfone ultrafiltration membranes for milk concentration. Polym. Adv. Technol., 16(10) (2005) 717–724. https://doi.org/10.1002/pat.644.
[28] L. Shen, X. Bian, X. Lu, L. Shi, Z. Liu, L. Chen, Z. Hou, and K. Fan, Preparation and characterization of ZnO/polyethersulfone (PES) hybrid membranes. Desalination, 293 (2012) 21–29. https://doi.org/10.1016/j.desal.2012.02.005.
[29] S. Hosseini, S. Madaeni, A. Khodabakhshi, The electrochemical characterization of ion exchange membranes in different electrolytic environments: investigation of concentration and pH effects. Sep. Sci. Technol., 47(3) (2012) 455–462. https://doi.org/10.1080/01496395.2011.625845.